Improved description of the $2\nu\beta\beta$-decay and a possibility to determine the effective axial-vector coupling constant

Fedor Šimkovic,[1,2,3] Rastislav Dvornický,[1,4] Dušan Štefánik,[1] and Amand Faessler[5]

[1]*Department of Nuclear Physics and Biophysics, Comenius University, Mlynská dolina F1, SK-842 48 Bratislava, Slovakia*

[2]*Boboliubov Laboratory of Theoretical Physics, JINR 141980 Dubna, Russia*

[3]*Czech Technical University in Prague, 128-00 Prague, Czech Republic*

[4]*Dzhelepov Laboratory of Nuclear Problems, JINR 141980 Dubna, Russia*

[5]*Institute of Theoretical Physics, University of Tuebingen, Auf der Morgenstelle 14, D-72076 Tuebingen, Germany*

(Received 30 November 2017; revised manuscript received 1 February 2018; published 13 March 2018)

An improved formalism of the two-neutrino double-beta decay ($2\nu\beta\beta$-decay) rate is presented, which takes into account the dependence of energy denominators on lepton energies via the Taylor expansion. Until now, only the leading term in this expansion has been considered. The revised $2\nu\beta\beta$-decay rate and differential characteristics depend on additional phase-space factors weighted by the ratios of $2\nu\beta\beta$-decay nuclear matrix elements with different powers of the energy denominator. For nuclei of experimental interest all phase-space factors are calculated by using exact Dirac wave functions with finite nuclear size and electron screening. For isotopes with measured $2\nu\beta\beta$-decay half-life the involved nuclear matrix elements are determined within the quasiparticle random-phase approximation with partial isospin restoration. The importance of correction terms to the $2\nu\beta\beta$-decay rate due to Taylor expansion is established and the modification of shape of single and summed electron energy distributions is discussed. It is found that the improved calculation of the $2\nu\beta\beta$-decay predicts slightly suppressed $2\nu\beta\beta$-decay background to the neutrinoless double-beta decay signal. Furthermore, an approach to determine the value of effective weak-coupling constant in nuclear medium $g_{\rm A}^{\rm eff}$ is proposed.

DOI: 10.1103/PhysRevC.97.034315

I. INTRODUCTION

The two-neutrino double beta decay ($2\nu\beta\beta$-decay) [1–3],

$$(A,Z) \to (A,Z+2) + 2e^- + 2\overline{\nu}_e, \tag{1}$$

a process fully consistent with the standard model of electroweak interaction, is the rarest process measured so far in nature. It has been observed in twelve even-even nuclei, in which single-β decay is energetically forbidden or strongly suppressed [4].

The $2\nu\beta\beta$-decay is a source of background in experiments looking for a signal of the neutrinoless double beta decay ($0\nu\beta\beta$-decay) [1–3],

$$(A,Z) \to (A,Z+2) + 2e^-, \tag{2}$$

the observation of which would prove that neutrinos are Majorana particles, i.e., their own antiparticles.

The inverse half-life of the $2\nu\beta\beta$-decay is commonly presented by the product of a phase-space factor $G^{2\nu}$, the fourth power of the effective axial-vector coupling constant $g_A^{\rm eff}$ and the $2\nu\beta\beta$-decay nuclear matrix element (NME) $M_{GT}^{2\nu}$ as follows:

$$\left(T_{1/2}^{2\nu}\right)^{-1} = \left(g_A^{\rm eff}\right)^4 \left|M_{GT}^{2\nu}\right|^2 G^{2\nu}. \tag{3}$$

The matrix element $M_{GT}^{2\nu}$, which value can be determined from the measured $2\nu\beta\beta$ half-life by making assumption about the value of $g_A^{\rm eff}$, plays an important role in understanding of the nuclear structure of double-beta-decay isotopes [5]. Its value is used to adjust the residual part of the nuclear Hamiltonian in the calculation of the $0\nu\beta\beta$-decay NME within the proton-neutron quasiparticle random-phase approximation (pnQRPA) [6,7]. With to this procedure, the results are only weakly sensitive to the size of the model space and the chosen type of NN interaction. So far, $2\nu\beta\beta$-decay NMEs have been calculated without the closure approximation only within the interacting shell model (ISM) [8] and the pnQRPA [9].

The measured single and summed electron differential decay rates of the $2\nu\beta\beta$-decay allow us to get valuable information concerning many interesting physical issues. In particular, from the shape of the summed electron distribution we get constraints on the Majoron mode of the $0\nu\beta\beta$-decay [10], the bosonic neutrino component [11], and violation of Lorentz invariance [12]. In addition, a reconstruction of individual electron energies and angular correlations in the NEMO3 experiment allow us to obtain information about the single-state dominance (SSD) and higher-state dominance (HSD) hypotheses discussing the importance of various contributions to the $2\nu\beta\beta$-decay NME from transitions through intermediate nuclear states [13,14].

Recently, significant progress has been achieved in double-beta-decay experiments. The $2\nu\beta\beta$-decay mode has been measured with high statistics in the GERDA (^{76}Ge) [15], NEMO3 (^{100}Mo) [16], CUORE (^{130}Te) [17], EXO (^{136}Xe) [18], and KamlandZEN (^{136}Xe) [19] experiments. As a consequence there is a request for more accurate description of the $2\nu\beta\beta$-decay process and corresponding differential characteristics. In this contribution we improve the theoretical description of the $2\nu\beta\beta$-decay process by taking into account the dependence

on lepton energies from the energy denominators of nuclear matrix elements, which has been neglected until now. In addition, a possibility to determine the effective axial-vector coupling constant $g_A^{\rm eff}$ is proposed.

II. IMPROVED FORMALISM FOR DESCRIPTION OF DOUBLE-BETA DECAY

In what follows we present improved formulas for the $2\nu\beta\beta$- and $0\nu\beta\beta$-decay half-lives in which the effect of the lepton energies in the energy denominator of NMEs is taken into account.

A. $2\nu\beta\beta$-decay rate

The inverse half-life of the $2\nu\beta\beta$-decay transition to the 0^+ ground state of the final nucleus takes the form

$$\left[T_{1/2}^{2\nu}\right]^{-1} = \frac{m_e}{8\pi^7 \ln 2}\left(G_\beta m_e^2\right)^4 \left(g_A^{\rm eff}\right)^4 I^{2\nu}, \tag{4}$$

where $G_\beta = G_F \cos\theta_C$ (G_F is Fermi constant and θ_C is the Cabibbo angle), m_e is the mass of the electron, and

$$\begin{aligned} I^{2\nu} = \frac{1}{m_e^{11}} &\int_{m_e}^{E_i-E_f-m_e} F_0(Z_f,E_{e_1}) p_{e_1} E_{e_1} dE_{e_1} \\ &\times \int_{m_e}^{E_i-E_f-E_{e_1}} F_0(Z_f,E_{e_2}) p_{e_2} E_{e_2} dE_{e_2} \\ &\times \int_0^{E_i-E_f-E_{e_1}-E_{e_2}} E_{\nu_1}^2 E_{\nu_2}^2 \mathcal{A}^{2\nu} dE_{\nu_1}. \end{aligned} \tag{5}$$

Here, $E_{\nu_2} = E_i - E_f - E_{e_1} - E_{e_2} - E_{\nu_1}$ due to energy conservation. E_i, E_f, E_{e_i} [$E_{e_i} = (p_{e_i}^2 + m_e^2)^{1/2}$], and E_{ν_i} (i = 1,2) are the energies of initial and final nuclei, electrons, and antineutrinos, respectively. $F(Z_f, E_{e_i})$ denotes relativistic Fermi function and $Z_f = Z + 2$. $\mathcal{A}^{2\nu}$ consists of products of the Gamow–Teller nuclear matrix elements (we neglect the contribution from the double Fermi transitions to the $2\nu\beta\beta$-decay rate), which depends on lepton energies [5]:

$$\mathcal{A}^{2\nu} = \left[\tfrac{1}{4}\left|M_{GT}^K + M_{GT}^L\right|^2 + \tfrac{1}{12}\left|M_{GT}^K - M_{GT}^L\right|^2\right],$$

where

$$M_{GT}^{K,L} = m_e \sum_n M_n \frac{E_n - (E_i+E_f)/2}{[E_n - (E_i+E_f)/2]^2 - \varepsilon_{K,L}^2}, \tag{6}$$

with

$$M_n = \langle 0_f^+ | \sum_m \tau_m^- \sigma_m | 1_n^+ \rangle \langle 1_n^+ | \sum_m \tau_m^- \sigma_m | 0_i^+ \rangle. \tag{7}$$

Here, $|0_i^+\rangle$, $|0_f^+\rangle$ are the 0^+ ground states of the initial and final even-even nuclei, respectively, and $|1_n^+\rangle$ are all possible states of the intermediate nucleus with angular momentum and parity $J^\pi = 1^+$ and energy $E_n(1^+)$. The lepton energies enter in the factors

$$\begin{aligned} \varepsilon_K &= (E_{e_2} + E_{\nu_2} - E_{e_1} - E_{\nu_1})/2, \\ \varepsilon_L &= (E_{e_1} + E_{\nu_2} - E_{e_2} - E_{\nu_1})/2. \end{aligned} \tag{8}$$

The maximal value of $|\varepsilon_K|$ and $|\varepsilon_L|$ is half of the Q value of the process [$\varepsilon_{K,L} \in (-Q/2, Q/2)$]. For $2\nu\beta\beta$-decay with energetically forbidden transitions to an intermediate nucleus ($E_n - E_i > -m_e$) the quantity $E_n - (E_i + E_f)/2 = Q/2 + m_e + (E_n - E_i)$ is always larger than half of the Q value.

The calculation of the $2\nu\beta\beta$-decay probability is usually simplified by an approximation

$$M_{GT}^{K,L} \simeq M_{GT}^{2\nu} = m_e \sum_n \frac{M_n}{E_n - (E_i+E_f)/2}, \tag{9}$$

which allows a separate calculation of the phase-space factor and nuclear matrix element.

The calculation of $M_{GT}^{2\nu}$ requires us to evaluate explicitly the matrix elements to and from the individual $|1_n^+\rangle$ states in the intermediate odd-odd nucleus. In the IBM calculation of this matrix element [20], the sum over virtual intermediate nuclear states is completed by closure after replacing $E_n - (E_i + E_f)/2$ by some average value E_{av}:

$$M_{GT}^{2\nu} \simeq \frac{m_e}{E_{av}} M_{GT-cl}^{2\nu}, \tag{10}$$

with

$$M_{GT-cl}^{2\nu} = \langle 0_f^+ | \sum_{m,n} \tau_m^- \tau_n^- \vec{\sigma}_m \cdot \vec{\sigma}_n | 0_i^+ \rangle. \tag{11}$$

The validity of the closure approximation is as good as the guess about the average energy to be used. This approximation might be justified, e.g., in the case there is a dominance of transition through a single state of the intermediate nucleus [21].

We get a more accurate expression for the $2\nu\beta\beta$-decay rate by performing the Taylor expansion in matrix elements $M_{GT}^{K,L}$ over the ratio $\varepsilon_{K,L}/[E_n - (E_i + E_f)/2]$. By limiting our consideration to the fourth power in ε we obtain

$$\left[T_{1/2}^{2\nu}\right]^{-1} \equiv \frac{\Gamma^{2\nu}}{\ln(2)} \simeq \frac{\Gamma_0^{2\nu} + \Gamma_2^{2\nu} + \Gamma_4^{2\nu}}{\ln(2)}, \tag{12}$$

where partial contributions to the full $2\nu\beta\beta$-decay width $\Gamma^{2\nu}$ associated with the leading $\Gamma_0^{2\nu}$, next-to-leading $\Gamma_2^{2\nu}$, and next-to-next-to-leading $\Gamma_4^{2\nu}$ orders in the Taylor expansion are given by

$$\begin{aligned} &\frac{\Gamma_0^{2\nu}}{\ln(2)} = \left(g_A^{\rm eff}\right)^4 \mathcal{M}_0 G_0^{2\nu}, \quad \frac{\Gamma_2^{2\nu}}{\ln(2)} = \left(g_A^{\rm eff}\right)^4 \mathcal{M}_2 G_2^{2\nu}, \\ &\frac{\Gamma_4^{2\nu}}{\ln(2)} = \left(g_A^{\rm eff}\right)^4 \left(\mathcal{M}_4 G_4^{2\nu} + \mathcal{M}_{22} G_{22}^{2\nu}\right). \end{aligned} \tag{13}$$

The phase-space factors are defined as

$$\begin{aligned} G_N^{2\nu} = \frac{c_{2\nu}}{m_e^{11}} &\int_{m_e}^{E_i-E_f-m_e} F_0(Z_f,E_{e_1}) p_{e_1} E_{e_1} dE_{e_1} \\ &\times \int_{m_e}^{E_i-E_f-E_{e_1}} F_0(Z_f,E_{e_2}) p_{e_2} E_{e_2} dE_{e_2} \\ &\times \int_0^{E_i-E_f-E_{e_1}-E_{e_2}} E_{\nu_1}^2 E_{\nu_2}^2 \mathcal{A}_N^{2\nu} dE_{\nu_1} \quad (N = 0,2,4,22), \end{aligned} \tag{14}$$

with $c_{2\nu} = m_e(G_\beta m_e^2)^4/(8\pi^7 \ln 2)$ and

$$\mathcal{A}_0^{2\nu} = 1, \quad \mathcal{A}_2^{2\nu} = \frac{\varepsilon_K^2 + \varepsilon_L^2}{(2m_e)^2},$$
$$\mathcal{A}_{22}^{2\nu} = \frac{\varepsilon_K^2 \varepsilon_L^2}{(2m_e)^4}, \quad \mathcal{A}_4^{2\nu} = \frac{\varepsilon_K^4 + \varepsilon_L^4}{(2m_e)^4}. \tag{15}$$

The products of nuclear matrix elements are given by

$$\mathcal{M}_0 = \left(M_{GT-1}^{2\nu}\right)^2, \quad \mathcal{M}_2 = M_{GT-1}^{2\nu} M_{GT-3}^{2\nu},$$
$$\mathcal{M}_{22} = \tfrac{1}{3}\left(M_{GT-3}^{2\nu}\right)^2,$$
$$\mathcal{M}_4 = \tfrac{1}{3}\left(M_{GT-3}^{2\nu}\right)^2 + M_{GT-1}^{2\nu} M_{GT-5}^{2\nu}, \tag{16}$$

where nuclear matrix elements take the forms

$$M_{GT-1}^{2\nu} \equiv M_{GT}^{2\nu},$$
$$M_{GT-3}^{2\nu} = \sum_n M_n \frac{4m_e^3}{[E_n - (E_i + E_f)/2]^3},$$
$$M_{GT-5}^{2\nu} = \sum_n M_n \frac{16m_e^5}{[E_n - (E_i + E_f)/2]^5}. \tag{17}$$

By introducing two ratios of nuclear matrix elements,

$$\xi_{31}^{2\nu} = \frac{M_{GT-3}^{2\nu}}{M_{GT-1}^{2\nu}}, \quad \xi_{51}^{2\nu} = \frac{M_{GT-5}^{2\nu}}{M_{GT-1}^{2\nu}}, \tag{18}$$

the $2\nu\beta\beta$-decay half-life,

$$\left[T_{1/2}^{2\nu\beta\beta}\right]^{-1} = \left(g_A^{\rm eff}\right)^4 \left|M_{GT-1}^{2\nu}\right|^2 \left\{G_0^{2\nu} + \xi_{31}^{2\nu} G_2^{2\nu} + \tfrac{1}{3}\left(\xi_{31}^{2\nu}\right)^2 G_{22}^{2\nu} + \left[\tfrac{1}{3}\left(\xi_{31}^{2\nu}\right)^2 + \xi_{51}^{2\nu}\right] G_4^{2\nu}\right\}, \tag{19}$$

is expressed with single NME ($M_{GT-1}^{2\nu}$) and two ratios of nuclear matrix elements ($\xi_{31}^{2\nu}$ and $\xi_{51}^{2\nu}$), which have to be calculated by means of nuclear structure theory, four phase-space factors ($G_0^{2\nu}$, $G_2^{2\nu}$, $G_{22}^{2\nu}$, and $G_4^{2\nu}$), which can be computed with a good accuracy, and the unknown parameter $g_A^{\rm eff}$.

B. $0\nu\beta\beta$-decay rate

The inverse lifetime of the $0\nu\beta\beta$ decay is commonly presented as a product of the total lepton number violating Majorana neutrino mass $m_{\beta\beta}$, the phase-space factor $G^{0\nu}$, the nuclear matrix element $M'^{0\nu}(g_A^{\rm eff})$, and the unquenched axial-vector coupling constant g_A ($g_A = 1.269$) in the fourth power as follows [3]:

$$\left(T_{1/2}^{0\nu}\right)^{-1} = \left|\frac{m_{\beta\beta}}{m_e}\right|^2 g_A^4 \left|M'^{0\nu}\left(g_A^{\rm eff}\right)\right|^2 G^{0\nu}, \tag{20}$$

where

$$G^{0\nu} = \frac{G_\beta^4 m_e^7}{32\pi^5 R^2 \ln(2)} \frac{1}{m_e^5} \int_{m_e}^{E_i - E_f - m_e} F_0(Z_f, E_{e_1}) \times p_{e_1} E_{e_1} F_0(Z_f, E_{e_2}) p_{e_2} E_{e_2} dE_{e_1}, \tag{21}$$

with $E_{e_2} = E_i - E_f - E_{e_1}$, $p_{e_i} = (E_{e_i}^2 - m_e^2)^{1/2}$ $(i = 1,2)$. The NME takes the form

$$M'^{0\nu}\left(g_A^{\rm eff}\right) = \frac{R}{2\pi^2 g_A^2} \sum_n \int e^{i\mathbf{p}\cdot(\mathbf{x}-\mathbf{y})} \times \frac{\langle 0_f^+ | J_L^{\mu\dagger}(\mathbf{x}) | n \rangle \langle n | J_{L\mu}^\dagger(\mathbf{y}) | 0_i^+ \rangle}{p(p + E_n - \frac{E_i - E_f}{2})} d^3p d^3x d^3y. \tag{22}$$

We note that the axial-vector $g_A^{\rm eff}(p^2)$ and induced pseudoscalar $g_P^{\rm eff}(p^2)$ form factors of nuclear hadron currents $J^{\mu\dagger}$ are "renormalized in the nuclear medium." The magnitude and origin of this renormalization is the subject of the analysis of many works, since it tends to increase the $0\nu\beta\beta$-decay half-life in comparison with the case in which this effect is absent [22,23].

In the derivation of the $0\nu\beta\beta$-decay rate in Eq. (20) the standard approximations were adopted: (i) A factorization of the phase-space factor and nuclear matrix element was achieved by an approximation in which electron wave functions were replaced by their values at the nuclear radius R. (ii) The dependence on lepton energies in energy denominators of the $0\nu\beta\beta$-decay NME was neglected.

Here, we go beyond the approximation (ii). The $0\nu\beta\beta$ nuclear matrix element contains a sum of two energy denominators:

$$\frac{1}{p_0 + E_n - E_i + E_{e_1}} + \frac{1}{p_0 + E_n - E_i + E_{e_2}}, \tag{23}$$

where $p = (p_0, \boldsymbol{p})$ is the four-momentum transferred by the Majorana neutrino [common for all neutrino mass eigenstates, since the neutrino masses m_i can be safely neglected in $p_0 = (\vec{p}^{\,2} + m_i^2)^{1/2} \approx |\vec{p}\,| \sim 100$ MeV]. By taking advantage of the energy conservation $E_i = E_f + E_{e_1} + E_{e_2}$ (the effect of nuclear recoil is disregarded) the approximation was adopted as follows:

$$\frac{2\left(p_0 + E_n - \frac{E_i + E_f}{2}\right)}{\left(p_0 + E_n - \frac{E_i + E_f}{2}\right)^2 - \varepsilon^2} \simeq \frac{2}{p_0 + E_n - \frac{E_i + E_f}{2}}, \tag{24}$$

with $\varepsilon = (E_{e_1} - E_{e_2})/2$. A more accurate expression for the $0\nu\beta\beta$-decay half-life is achieved by taking into account next term in the Taylor expansion over the quantity $\varepsilon^2/[p_0 + E_n - (E_i + E_f)/2]^2$ in Eq. (24). We end up with

$$\left(T_{1/2}^{0\nu}\right)^{-1} = \left|\frac{m_{\beta\beta}}{m_e}\right|^2 g_A^4 \left|M'^{0\nu}_1\right|^2 \left(G_0^{0\nu} + 2\xi_{31}^{0\nu} G_2^{0\nu}\right), \tag{25}$$

where

$$G_N^{0\nu} = \frac{G_\beta^4 m_e^7}{32\pi^5 R^2 \ln(2)} \frac{1}{m_e^5} \int_{m_e}^{E_i - E_f - m_e} \mathcal{A}_N^{0\nu} F_0(Z_f, E_{e_1}) \times p_{e_1} E_{e_1} F_0(Z_f, E_{e_2}) p_{e_2} E_{e_2} dE_{e_1}, \tag{26}$$

with

$$\mathcal{A}_0^{0\nu} = 1, \quad \mathcal{A}_2^{0\nu} = \varepsilon^2/(2m_e)^2. \tag{27}$$

TABLE I. Phase-space factors $G^{2\nu}_{0,2,22,4}$ ($G^{0\nu}_{0,2}$) entering the $2\nu\beta\beta$-decay ($0\nu\beta\beta$-decay) rate in Eq. (12) [Eq. (25)]. The radial wave functions g_{-1} and f_{+1} of an electron, which constitute the Fermi function in Eq. (31), were calculated in two approximation schemes: (A) The standard approximation of Doi *et al.* [2]. (B) The exact Dirac wave functions with finite nuclear size and electron screening [25].

		$2\nu\beta\beta$-decay				$0\nu\beta\beta$-decay	
Nucleus	Elec. w. f.	$G^{2\nu}_0$ [yr^{-1}]	$G^{2\nu}_2$ [yr^{-1}]	$G^{2\nu}_4$ [yr^{-1}]	$G^{2\nu}_{22}$ [yr^{-1}]	$G^{0\nu}_0$ [yr^{-1}]	$G^{0\nu}_2$ [yr^{-1}]
^{48}Ca	A	1.608×10^{-17}	1.372×10^{-17}	1.484×10^{-17}	3.297×10^{-18}	2.641×10^{-14}	2.284×10^{-14}
	B	1.534×10^{-17}	1.307×10^{-17}	7.064×10^{-18}	3.140×10^{-18}	2.489×10^{-14}	2.150×10^{-14}
^{76}Ge	A	5.278×10^{-20}	1.113×10^{-20}	2.924×10^{-21}	6.898×10^{-22}	2.613×10^{-15}	6.269×10^{-16}
	B	4.816×10^{-20}	1.015×10^{-20}	1.332×10^{-21}	6.284×10^{-22}	2.370×10^{-15}	5.670×10^{-16}
^{82}Se	A	1.763×10^{-18}	7.805×10^{-19}	4.333×10^{-19}	9.912×10^{-20}	1.147×10^{-14}	5.449×10^{-15}
	B	1.591×10^{-18}	7.037×10^{-19}	1.952×10^{-19}	8.931×10^{-20}	1.020×10^{-14}	4.830×10^{-15}
^{96}Zr	A	7.777×10^{-18}	4.292×10^{-18}	2.974×10^{-18}	6.774×10^{-19}	2.423×10^{-14}	1.422×10^{-14}
	B	6.796×10^{-18}	3.745×10^{-18}	1.296×10^{-18}	5.907×10^{-19}	2.067×10^{-14}	1.209×10^{-14}
^{100}Mo	A	3.818×10^{-18}	1.747×10^{-18}	1.001×10^{-18}	2.301×10^{-19}	1.890×10^{-14}	9.357×10^{-15}
	B	3.303×10^{-18}	1.509×10^{-18}	4.320×10^{-19}	1.986×10^{-19}	1.599×10^{-14}	7.886×10^{-15}
^{110}Pd	A	1.629×10^{-19}	3.405×10^{-20}	8.832×10^{-21}	2.115×10^{-21}	5.783×10^{-15}	1.408×10^{-15}
	B	1.379×10^{-19}	2.881×10^{-20}	3.735×10^{-21}	1.789×10^{-21}	4.833×10^{-15}	1.172×10^{-15}
^{116}Cd	A	3.314×10^{-18}	1.318×10^{-18}	6.546×10^{-19}	1.522×10^{-19}	2.064×10^{-14}	9.061×10^{-15}
	B	2.763×10^{-18}	1.097×10^{-18}	2.722×10^{-19}	1.266×10^{-19}	1.677×10^{-14}	7.334×10^{-15}
^{124}Sn	A	6.717×10^{-19}	1.794×10^{-19}	5.954×10^{-20}	1.414×10^{-20}	1.124×10^{-14}	3.442×10^{-15}
	B	5.534×10^{-19}	1.476×10^{-19}	2.448×10^{-20}	1.163×10^{-20}	9.077×10^{-15}	2.768×10^{-15}
^{128}Te	A	3.314×10^{-22}	1.314×10^{-23}	6.409×10^{-25}	1.688×10^{-25}	7.263×10^{-16}	3.875×10^{-17}
	B	2.699×10^{-22}	1.070×10^{-23}	2.609×10^{-25}	1.374×10^{-25}	5.904×10^{-16}	3.145×10^{-17}
^{130}Te	A	1.885×10^{-18}	6.112×10^{-19}	2.467×10^{-19}	5.812×10^{-20}	1.807×10^{-14}	6.619×10^{-15}
	B	1.530×10^{-18}	4.953×10^{-19}	9.985×10^{-20}	4.707×10^{-20}	1.428×10^{-14}	5.212×10^{-15}
^{134}Xe	A	2.924×10^{-22}	1.066×10^{-23}	4.773×10^{-25}	1.264×10^{-25}	7.613×10^{-16}	3.761×10^{-17}
	B	2.347×10^{-22}	8.553×10^{-24}	1.915×10^{-25}	1.014×10^{-25}	6.100×10^{-16}	3.008×10^{-17}
^{136}Xe	A	1.793×10^{-18}	5.516×10^{-19}	2.110×10^{-19}	4.994×10^{-20}	1.881×10^{-14}	6.590×10^{-15}
	B	1.433×10^{-18}	4.404×10^{-19}	8.417×10^{-20}	3.986×10^{-20}	1.464×10^{-14}	5.107×10^{-15}
^{150}Nd	A	4.817×10^{-17}	2.731×10^{-17}	1.937×10^{-17}	4.479×10^{-18}	8.827×10^{-14}	5.462×10^{-14}
	B	3.642×10^{-17}	2.061×10^{-17}	7.295×10^{-18}	3.380×10^{-18}	6.339×10^{-14}	3.903×10^{-14}

The additional term in the $0\nu\beta\beta$-decay rate in Eq. (25) is weighted by the ratio $\xi^{0\nu}_{31}$,

$$\xi^{0\nu}_{31} = \frac{M'^{0\nu}_3\left(g_A^{\rm eff}\right)}{M'^{0\nu}_1\left(g_A^{\rm eff}\right)}, \tag{28}$$

of two NMEs defined as follows:

$$\begin{aligned} M'^{0\nu}_1\left(g_A^{\rm eff}\right) &\equiv M'^{0\nu}\left(g_A^{\rm eff}\right) \\ M'^{0\nu}_3\left(g_A^{\rm eff}\right) &= \frac{R}{2\pi^2 g_A^2}(2m_e)^2 \sum_n \int e^{i\mathbf{p}\cdot(\mathbf{x}-\mathbf{y})} \\ &\quad \times \frac{\langle 0^+_f|J^{\mu\dagger}_L(\mathbf{x})|n\rangle\langle n|J^{\dagger}_{L\mu}(\mathbf{y})|0^+_i\rangle}{p(p+E_n-\frac{E_i-E_f}{2})^3} \\ &\quad \times d^3p d^3x d^3y. \end{aligned} \tag{29}$$

III. CALCULATIONS AND RESULTS

A. Phase-space factors and quasiparticle random-phase approximation nuclear matrix elements

The $2\nu\beta\beta$- and $0\nu\beta\beta$-phase-space factors presented in the previous section are associated with the $s_{1/2}$ electron wave function distorted by the Coulomb field:

$$\Psi^{(s_{1/2})}(E_e,\boldsymbol{r}) = \begin{pmatrix} g_{-1}(E_e,r)\chi_s \\ f_{+1}(E_e,r)(\sigma\cdot\hat{\mathbf{p}}_\mathbf{e})\chi_s \end{pmatrix}, \tag{30}$$

where E_e and $\boldsymbol{p}_e$ are the electron energy and momentum, respectively. $\hat{p}_e = \boldsymbol{p}_e/|\boldsymbol{p}_e|$ and $r = |\boldsymbol{r}|$ is the radial coordinate of the position of the electron. The values of the radial functions $g_{-1}(E_e,r)$ and $f_{+1}(E_e,r)$ at nuclear radius $r = R$ constitute the Fermi function as follows:

$$F_0(Z,E_e) = g^2_{-1}(E_e,R) + f^2_{+1}(E_e,R). \tag{31}$$

Two different approximation schemes for the calculation of radial wave functions $g_{-1}(E_e,R)$ and $f_{+1}(E_e,R)$ are considered.

1. The approximation scheme A.

The relativistic electron wave function in a uniform charge distribution in nucleus is considered. The lowest terms in the power expansion in r/R are taken into account. The Fermi function takes the form

$$F_0 = \left[\frac{\Gamma(3)}{\Gamma(1)\Gamma(1+2\gamma_0)}\right]^2 (2p_eR)^{2(\gamma_0-1)}e^{\pi y}|\Gamma(\gamma_0+iy)|^2, \tag{32}$$

where $\gamma_0 = [1-(\alpha)^2]^{1/2}$ and $y = \alpha Z\frac{\varepsilon}{p_e}$.

2. The approximation scheme B.

The exact Dirac wave functions with finite nuclear size and electron screening are used [25]. The effect of screening of atomic electrons is taken into account by the Thomas–Fermi

TABLE II. The $2\nu\beta\beta$- and $0\nu\beta\beta$-decay nuclear matrix elements and ratios of nuclear matrix elements [see Eqs. (18) and (28)] calculated within the *pn*QRPA with partial isospin restoration [24]. $P_0^{2\nu}$, $P_2^{2\nu}$, and $P_4^{2\nu}$ are the leading first-, second-, and third-order contributions to the $2\nu\beta\beta$-decay rate in the Taylor expansion. $T_{1/2}^{2\nu-exp}$ is the averaged value of the $2\nu\beta\beta$-decay half-life [4] considered in the calculation of the $2\nu\beta\beta$-decay NMEs. $g_A^{\rm eff}$ is the effective axial-vector coupling constant.

	$2\nu\beta\beta$-decay										$0\nu\beta\beta$-decay	
Nucleus	$g_A^{\rm eff}$	$M_{GT-1}^{2\nu}$	$M_{GT-3}^{2\nu}$	$M_{GT-5}^{2\nu}$	$\xi_{31}^{2\nu}$	$\xi_{51}^{2\nu}$	$P_0^{2\nu}$	$P_2^{2\nu}$	$P_4^{2\nu}$	$T_{1/2}^{2\nu-exp}$ [yr]	$M'^{0\nu}_1$	$\xi_{31}^{0\nu}$
^{48}Ca	0.800	0.0553	0.0105	0.00163	0.1891	0.0295	0.8456	0.1362	0.0182	4.4×10^{19}	0.4066	6.463×10^{-4}
	1.000	0.0352	0.00723	0.00105	0.2055	0.0298	0.8346	0.1461	0.0193		0.4543	6.732×10^{-4}
	1.269	0.0214	0.00539	0.00075	0.2514	0.0351	0.8036	0.1722	0.0242		0.5288	6.814×10^{-4}
^{76}Ge	0.800	0.175	0.0214	0.00445	0.1220	0.0254	0.9741	0.0250	0.0009	1.65×10^{21}	3.1822	2.629×10^{-4}
	1.000	0.111	0.0133	0.00263	0.1204	0.0237	0.9745	0.0247	0.0008		3.8830	2.484×10^{-4}
	1.269	0.689	0.00716	0.00716	0.1040	0.0170	0.9780	0.0214	0.0006		5.1527	2.282×10^{-4}
^{82}Se	0.800	0.124	0.0216	0.00645	0.1745	0.0521	0.9213	0.0711	0.0076	0.92×10^{20}	2.7859	2.243×10^{-4}
	1.000	0.0795	0.0129	0.00355	0.1620	0.0446	0.9271	0.0664	0.0065		3.4668	2.146×10^{-4}
	1.269	0.0498	0.00643	0.00136	0.1290	0.0272	0.9421	0.0538	0.0041		4.6511	2.020×10^{-4}
^{96}Zr	0.800	0.1146	0.0348	0.00885	0.3036	0.0773	0.8399	0.1405	0.0195	2.3×10^{19}	1.9299	6.872×10^{-4}
	1.000	0.0718	0.273	0.00697	0.3800	0.0971	0.8056	0.1687	0.0257		2.2449	8.552×10^{-4}
	1.269	0.0431	0.0220	0.00564	0.5101	0.1309	0.7518	0.2113	0.0369		2.8163	1.009×10^{-3}
^{100}Mo	0.800	0.292	0.123	0.0453	0.4230	0.1553	0.8163	0.1578	0.0259	7.1×10^{18}	3.4765	8.297×10^{-4}
	1.000	0.184	0.0876	0.0322	0.4752	0.1745	0.7972	0.1731	0.0297		4.1737	8.997×10^{-4}
	1.269	0.112	0.0633	0.0233	0.5646	0.2075	0.7661	0.1976	0.0363		5.3824	8.908×10^{-4}
^{116}Cd	0.800	0.1653	0.0478	0.0142	0.2890	0.0857	0.8872	0.1018	0.0110	2.87×10^{19}	2.5488	4.930×10^{-4}
	1.000	0.1053	0.0327	0.00972	0.3102	0.0923	0.8796	0.1083	0.0121		3.0859	5.240×10^{-4}
	1.269	0.0651	0.0219	0.00654	0.3370	0.1000	0.8702	0.1164	0.0134		4.0381	4.998×10^{-4}
^{130}Te	0.800	0.0466	0.00873	0.00239	0.1873	0.0512	0.9389	0.0569	0.0042	6.9×10^{20}	2.4122	4.830×10^{-4}
	1.000	0.0298	0.00577	0.00144	0.1937	0.0482	0.9371	0.0588	0.0041		2.9617	2.629×10^{-4}
	1.269	0.0185	0.00373	0.00078	0.2015	0.0420	0.9352	0.0610	0.0038		3.9026	1.488×10^{-4}
^{136}Xe	0.800	0.0268	0.00706	0.00232	0.2637	0.0866	0.9190	0.0745	0.0065	2.19×10^{21}	1.3425	1.608×10^{-4}
	1.000	0.0170	0.00526	0.00169	0.3098	0.0995	0.9059	0.0863	0.0078		1.6525	1.561×10^{-4}
	1.269	0.0104	0.00403	0.00126	0.3867	0.1207	0.8848	0.1051	0.0101		2.1841	1.509×10^{-4}

approximation. The numerical calculation is accomplished by the subroutine package RADIAL [26].

In Table I the $2\nu\beta\beta$- and $0\nu\beta\beta$-decay phase-space factors calculated within approximations A and B are presented for 13 isotopes of experimental interest. We see that all phase-space factors calculated with exact relativistic electron wave functions (the approximation scheme B) are smaller in comparison with those obtained in approximation scheme A. We note that, in both approximation schemes, the factorization of phase-space factors and nuclear matrix elements is achieved by considering radial electron wave functions at the nuclear radius and the difference between them is due to a different treatment of the Coulomb interaction.

In what follows, entries B from Table I will be used in the calculation of the $2\nu\beta\beta$ differential characteristics and decay rates.

B. Nuclear matrix elements

The $2\nu\beta\beta$- and $0\nu\beta\beta$-decay nuclear matrix elements [see Eqs. (17) and (29)] are calculated within the proton-neutron quasiparticle random-phase approximation (QRPA) with isospin restoration [24]. They were obtained by considering the same model spaces and mean fields as in Ref. [24]. The G-matrix elements of a realistic Argonne V18 nucleon-nucleon potential are considered. By using the improved theoretical description of the $2\nu\beta\beta$-decay rate in Eqs. (12)–(17), the isoscalar neutron-proton interaction of the nuclear Hamiltonian is adjusted to reproduce correctly the average $2\nu\beta\beta$-decay half-live [4] for each nucleus and each $g_A^{\rm eff}$.

In Table II the calculated $2\nu\beta\beta$-deacy NMEs are presented for $g_A^{\rm eff} = 0.8$, 1.0, and 1.269 (unquenched value). We see that, for all isotopes, the inequality $M_{GT-1}^{2\nu} > M_{GT-3}^{2\nu} > M_{GT-5}^{2\nu}$ is valid. The ratios of nuclear matrix elements $\xi_{31}^{2\nu}$, $\xi_{51}^{2\nu}$, and $\xi^{0\nu}$ depend only weakly on $g_A^{\rm eff}$. The largest values $\xi_{31}^{2\nu} = 0.56$ and $\xi_{51}^{2\nu} = 0.21$ are in the case ^{100}Mo.

The ratio $\xi_{31}^{2\nu}$ of nuclear matrix elements $M_{GT-3}^{2\nu}$ and $M_{GT-1}^{2\nu}$ [see Eq. (18)] is an important quantity due to a different structure of both nuclear matrix elements. This fact is displayed in Fig. 1 (Fig. 2), where a running sum of matrix elements $M_{GT-1}^{2\nu}$ and $M_{GT-3}^{2\nu}$ is plotted as a function of the excitation energy $E_{\rm ex}$ counted from the ground state of the intermediate nucleus for the $2\nu\beta\beta$-decay of ^{76}Ge, ^{82}Se, ^{96}Zr, and ^{100}Mo (^{48}Ca, ^{116}Cd, ^{130}Te, and ^{136}Xe). The results were obtained within the QRPA with partial isospin restoration [24]. By glancing at these figures we see that matrix element $M_{GT-3}^{2\nu}$ is determined by transitions through the lightest states of the intermediate nucleus unlike $M_{GT-1}^{2\nu}$, which depends also on the transitions through higher-lying states even from the region of Gamow–Teller resonance and a mutual cancellation among different contributions.

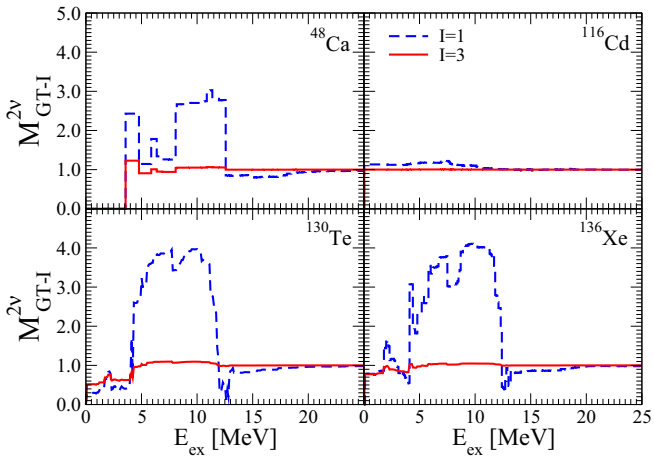

FIG. 1. Running sum of the $2\nu\beta\beta$-decay NMEs $M^{2\nu}_{GT-1}$ and $M^{2\nu}_{GT-3}$ [see Eq. (17)] for ^{48}Ca, ^{116}Cd, ^{130}Te, and ^{136}Xe (normalized to unity) as a function of the excitation energy $E_{\rm ex}$ counted from the ground state of intermediate nucleus. Calculations were performed within the proton-neutron QRPA with isospin restoration [24]. Results are obtained with Argonne V18 potential and for unquenched axial-vector coupling constant $g_A = 1.269$.

The convergence of the Taylor expansion of the $2\nu\beta\beta$-decay rate [see Eqs. (12)–(17)] depends on values of the original $M^{2\nu}_{GT-1}$ and the new $M^{2\nu}_{GT-3,5}$ nuclear matrix elements. Recall that the powers of $\varepsilon_{K,L}$ are included in the generalized phase-space factors $G^{2\nu}_{0,2,22,4}$ and the denominators are included in the new nuclear matrix elements $M^{2\nu}_{GT-3,5}$. The leading first- $P^{2\nu}_0$, second- $P^{2\nu}_2$, and third-order $P^{2\nu}_4$ term contributions to the $2\nu\beta\beta$-decay rate in the Taylor expansion normalized to the full decay rate are defined as

$$P^{2\nu}_I = \frac{\Gamma^{2\nu}_I}{\Gamma^{2\nu}}, \tag{33}$$

with $I = 0$, 2, and 4. Their values calculated with help of the $2\nu\beta\beta$-decay NMEs evaluated within the QRPA with partial restoration of isospin symmetry [24] are shown in Table II. We notice a good convergence of contributions to the $2\nu\beta\beta$-decay

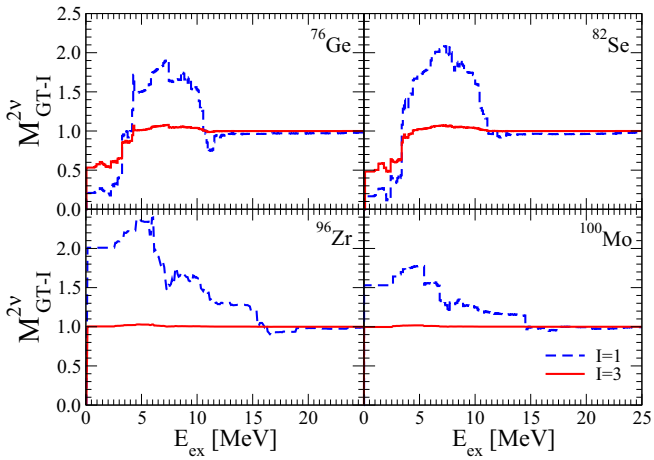

FIG. 2. The same as Fig. 1 but for the $2\nu\beta\beta$-decay of ^{76}Ge, ^{82}Se, ^{96}Zr, and ^{100}Mo.

rate due to the Taylor expansion. The size of these corrections depends on a given isotope. The largest value of about 25% is found by using ^{100}Mo.

In Table II the calculated $0\nu\beta\beta$-decay nuclear matrix elements are presented as well. They were obtained under the common assumption that the same $g^{\rm eff}_A$ governs both modes of double-beta decay [3,24]. The modification of the $2\nu\beta\beta$-decay rate due to the Taylor expansion has only negligible effect on the calculation of the $0\nu\beta\beta$-decay NMEs $M'^{0\nu}_{1,3}$ in the context of adjusting the particle-particle interaction strength.

By glancing at Table II we see that the value of $\xi^{0\nu}_{31}$ is very small; namely, significantly smaller as $\xi^{2\nu}_{31}$, as the average momentum of neutrino entering the energy denominator in Eq. (24) is about two orders of magnitude larger when compared with the maximal value ε, which is $Q/2$. Clearly, in the case of $0\nu\beta\beta$-decay the convergence of the Taylor expansion of the decay rate is fast and the standard approach given by the leading term in the Taylor expansion is well justified.

C. Energy distributions of emitted electrons

The NEMO3 experiment, which ran for seven years before it stopped taking data in 2010, measured the $2\nu\beta\beta$-decay of ^{100}Mo with very high statistics of about 1 million events [16]. Due to high statistics of about tens of thousands of events, the currently running EXO [18], KamLAND-Zen [19] (^{136}Xe), and GERDA (^{76}Ge) [15] experiments allow precise determination of the $2\nu\beta\beta$-decay energy distributions as well. A similar statistics is expected to be achieved also by the CUORE (^{130}Te) experiment, which has started taking data recently. New perspectives for analysis of $2\nu\beta\beta$-decay differential characteristics will be opened by the next generation of double-beta decay experiments like SuperNEMO, nEXO, and Legend, which will contain significantly larger amount of double-beta decay radioactive source [3,27].

By considering the leading first- and second-order terms in the Taylor expansion for the single and summed electron differential decay rate normalized to the full decay rate we get

$$\frac{1}{\Gamma^{2\nu}}\frac{d\Gamma^{2\nu}}{dT_e} \simeq \frac{1}{\Gamma^{2\nu}}\left(\frac{d\Gamma^{2\nu}_0}{dT_e} + \frac{d\Gamma^{2\nu}_2}{dT_e}\right) = \frac{1}{\left(G^{2\nu}_0 + \xi^{2\nu}_{31} G^{2\nu}_2\right)}\left(\frac{dG_0}{dT_e} + \xi^{2\nu}_{31}\frac{dG_2}{dT_e}\right), \tag{34}$$

$$\frac{1}{\Gamma^{2\nu}}\frac{d\Gamma^{2\nu}}{dT_{ee}} \simeq \frac{1}{\Gamma^{2\nu}}\left(\frac{d\Gamma^{2\nu}_0}{dT_{ee}} + \frac{d\Gamma^{2\nu}_2}{dT_{ee}}\right) = \frac{1}{\left(G^{2\nu}_0 + \xi^{2\nu}_{31} G^{2\nu}_2\right)}\left(\frac{dG_0}{dT_{ee}} + \xi^{2\nu}_{31}\frac{dG_2}{dT_{ee}}\right), \tag{35}$$

where

$$\frac{dG^{2\nu}_N}{dT_{e_1}} = \frac{c_{2\nu}}{m^{11}_e} F_0(Z_f, E_{e_1}) p_{e_1} E_{e_1} \times \int_0^{Q-T_{e_1}} F_0(Z_f, E_{e_2}) p_{e_2} E_{e_2} I_N(T_{e_1}, T_{e_2}) dT_{e_2},$$

$$\frac{dG^{2\nu}_N}{dT_{ee}} = \frac{c_{2\nu}}{m^{11}_e}\frac{T_{ee}}{Q}\int_0^{Q} F_0(Z_f, E_{e_1}) p_{e_1} E_{e_1} \times F_0(Z_f, E_{e_2}) p_{e_2} E_{e_2} I_N(T_{e_1}, T_{e_2}) dV \tag{36}$$

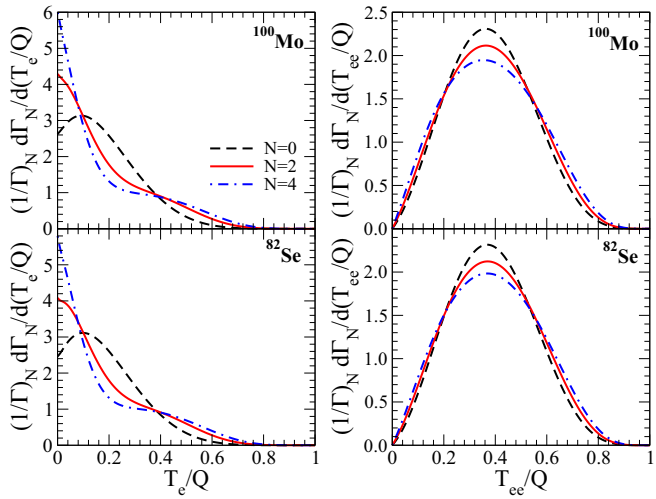

FIG. 3. Partial differential decay rates $(1/\Gamma_0)d\Gamma_0/dT_e$, $(1/\Gamma_2)d\Gamma_2/dT_e$, and $(1/\Gamma_4)d\Gamma_4/dT_e$ normalized to corresponding partial decay rate vs kinetic energy of a single electron T_e (in units of Q value) (left panels) and the partial differential decay rates $(1/\Gamma_0)d\Gamma_0/dT_{ee}$, $(1/\Gamma_2)d\Gamma_2/dT_{ee}$, and $(1/\Gamma_4)d\Gamma_4/dT_{ee}$ normalized to corresponding partial decay rate vs the sum of kinetic energies of emitted electrons T_{ee} (in units of Q value) (right panels) for the $2\nu\beta\beta$-decay of ^{82}Se and ^{100}Mo to the ground state of the final nucleus. The energy distributions are normalized to unity to see how their shapes differ.

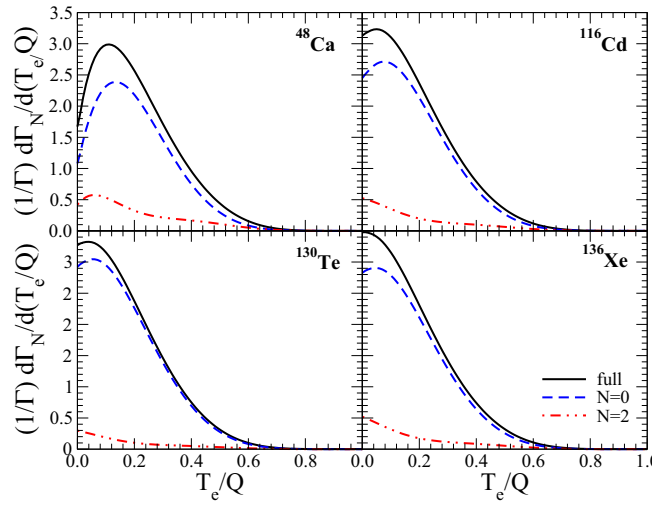

FIG. 4. The full differential decay rate $(1/\Gamma)d\Gamma/dT_e$ and partial differential decay rates $(1/\Gamma)d\Gamma_0/dT_e$ and $(1/\Gamma)d\Gamma_2/dT_e$ normalized by the full decay rate vs the kinetic energy of a single electron T_e (in units of Q value) for the $2\nu\beta\beta$-decay of ^{48}Ca, ^{116}Cd, ^{130}Te, and ^{136}Xe.

$(N = 0, 2)$, with

$$I_N(T_{e_1}, T_{e_2}) = \int_0^{Q-T_{e_1}-T_{e_2}} E_{\nu_1}^2 E_{\nu_2}^2 \mathcal{A}_N^{2\nu} dE_{\nu_1}, \qquad (37)$$

and

$$T_{ee} = T_{e_1} + T_{e_2}, \quad V = Q\frac{T_{e_2}}{T_{e_1} + T_{e_2}}. \qquad (38)$$

Here, $E_{\nu_2} = E_i - E_f - E_{e_1} - E_{e_1} - E_{\nu_1}$ is determined by energy conservation. T_{ee} is a sum of kinetic energies of both electrons (T_{e_1} and T_{e_2}), and T_e represents the kinetic energy of any of two emitted electrons.

The single and summed electron differential decay rates normalized to the full width in Eqs. (34) and (35) contain one unknown parameter; namely, the ratio $\xi_{31}^{2\nu}$. We note that partial contributions to the full differential decay rate in Eq. (34) [Eq. (35)] exhibit different behavior as a function of T_e (T_{ee}). This fact is displayed in Fig. 3, where single and summed electron partial differential decay rates normalized to the partial width (i.e., all energy distributions are normalized to unity and do not depend on any NME) are presented for the $2\nu\beta\beta$-decay of ^{82}Se and ^{100}Mo. The difference in distributions corresponding to the leading- and first-order terms in the Taylor expansion is apparent especially in the case of single-electron energy distribution. Due to this phenomenon there is a possibility to deduce ratio $\xi_{31}^{2\nu}$ from the measured energy distributions.

For the *pn*QRPA value of the parameter $\xi_{31}^{2\nu}$ (see Table II) the full differential decay rate $(1/\Gamma^{2\nu})d\Gamma^{2\nu}/dT_e$ and partial differential decay rates $(1/\Gamma^{2\nu})d\Gamma_0^{2\nu}/dT_e$, $(1/\Gamma^{2\nu})d\Gamma_2^{2\nu}/dT_e$ normalized by the full decay rate are presented as function of the kinetic energy of a single electron T_e [sum of kinetic energy of both electrons T_{ee} for the eight $2\nu\beta\beta$-decay isotopes in Figs. 4 and 5 (6 and 7)]. We see that the largest contribution from the additional term due to Taylor expansion to the full differential decay rate is found by the $2\nu\beta\beta$-decay of ^{100}Mo, ^{96}Zr, ^{48}Ca, ^{116}Cd, and ^{136}Xe. These isotopes are good candidates to measure $\xi_{31}^{2\nu}$ in double-beta-decay experiments.

By assuming $\xi_{13}^{2\nu} = 0.0$, 0.4, and 0.8. the single-electron energy distribution and summed electron energy spectrum normalized by the full decay rate for $2\nu\beta\beta$-decay of ^{82}Se and ^{100}Mo are presented in Fig. 8. We see that corresponding curves are close to each other and that high statistics of the $2\nu\beta\beta$-decay experiment is needed to deduce information about

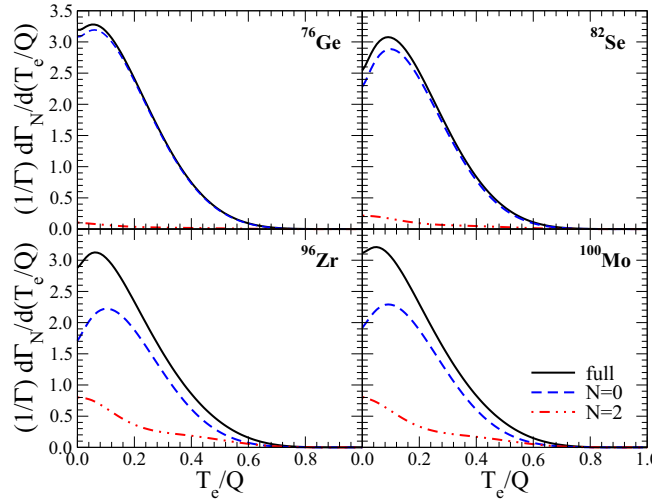

FIG. 5. The same as Fig. 4 but for the $2\nu\beta\beta$-decay of ^{76}Ge, ^{82}Se, ^{96}Zr, and ^{100}Mo.

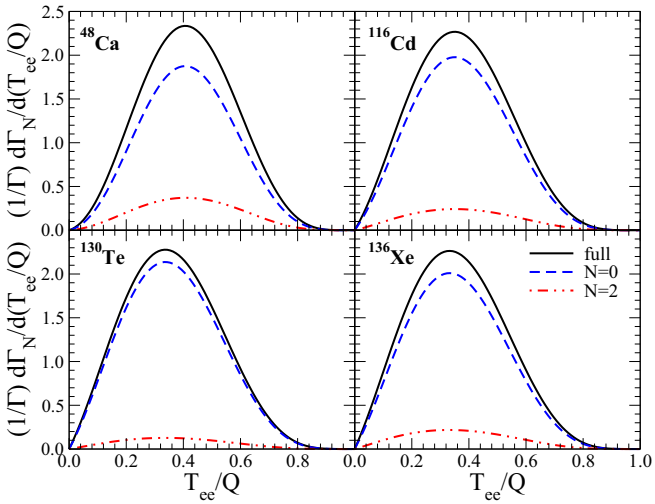

FIG. 6. The full differential decay rate $(1/\Gamma)d\Gamma/dT_e$ and partial differential decay rates $(1/\Gamma)d\Gamma_0/dT_e$ and $(1/\Gamma)d\Gamma_2/dT_e$ normalized by the full decay rate vs the sum of kinetic energies of emitted electrons T_{ee} (in units of Q value) for the $2\nu\beta\beta$-decay of ^{48}Ca, ^{116}Cd, ^{130}Te, and ^{136}Xe.

the ratio of nuclear matrix elements $\xi_{13}^{2\nu}$ from the data. The study performed within the NEMO3 experiment [28] with respect to the SSD versus the HSD hypothesis [13,14] has shown that it is feasible. It might be that the high statistics achieved by the GERDA [15], CUORE [17], EXO (^{136}Xe), and KamLAND-Zen (^{136}Xe) experiments is sufficient to conclude about the value of $\xi_{13}^{2\nu}$ for the measured $2\nu\beta\beta$-decay transition.

For some of future double-beta decay experiments the $2\nu\beta\beta$-decay is considered as important background for the signal of the $0\nu\beta\beta$-decay, e.g., in the case of the SuperNEMO experiment. In Fig. 9 the endpoint of the spectrum of the differential decay rate normalized by the full decay rate $(1/\Gamma)d\Gamma/dT$ as a function of the sum of kinetic energy of emitted electrons $T = (E_{e_1} + E_{e_2} - 2m_e)$ is presented for the

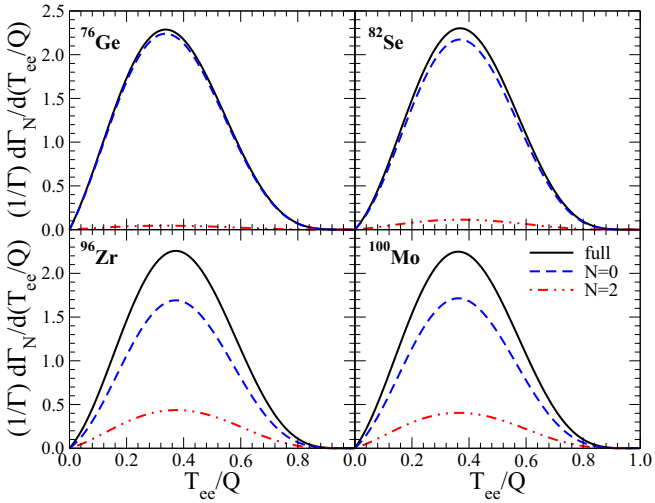

FIG. 7. The same as Fig. 6 for the $2\nu\beta\beta$-decay of ^{76}Ge, ^{82}Se, ^{96}Zr, and ^{100}Mo.

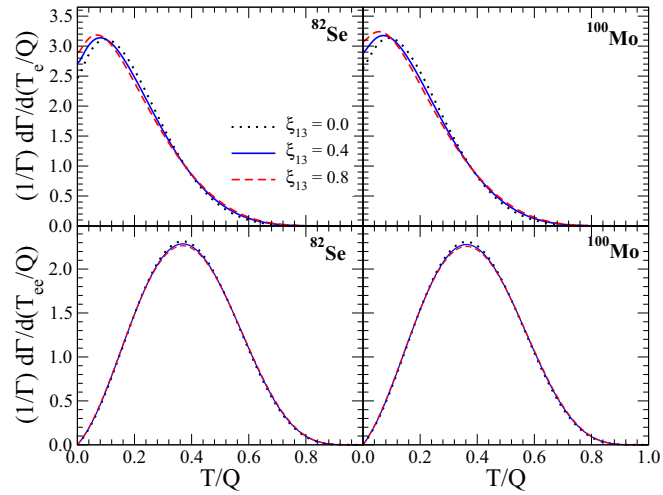

FIG. 8. Differential decay rates $(1/\Gamma)d\Gamma/d(T_e/Q)$ (upper panels) and $(1/\Gamma)d\Gamma/d(T_{ee}/Q)$ (lower panels) normalized by the full decay rate Γ vs kinetic energy of a single electron $T = T_e$ and the sum of kinetic energies of emitted electrons $T = T_{ee}$ (in units of Q value), respectively. Results are presented for the $2\nu\beta\beta$-decay of ^{82}Se (left panels) and ^{100}Mo (right panels) by assuming $\xi_{13}^{2\nu} = 0.0$, 0.40, and 0.8.

$2\nu\beta\beta$-decay of ^{82}Se and ^{100}Mo. The results were obtained with the common and improved theoretical expressions for the $2\nu\beta\beta$-decay rate. We see that, by considering the revised formula, the number of the $2\nu\beta\beta$-decay events close to the end of spectra is slightly suppressed in comparison with previous expectations, which is apparent especially in the case of the $2\nu\beta\beta$-decay of ^{100}Mo.

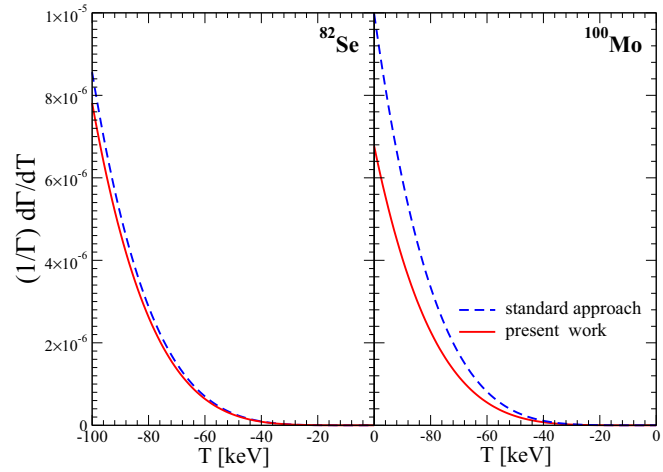

FIG. 9. The endpoint of the spectrum of the differential decay rate normalized to the full decay rate $(1/\Gamma)d\Gamma/dT$ vs the sum of kinetic energy of emitted electrons $T = (E_{e_1} + E_{e_2} - 2m_e)$ for the $2\nu\beta\beta$-decay of ^{82}Se and ^{100}Mo. The calculation with the standard (leading term in Taylor expansion) and improved (present work) theoretical description of the $2\nu\beta\beta$-decay rate. The considered ratios $\xi_{31}^{2\nu}$ and $\xi_{51}^{2\nu}$ are those calculated within the QRPA with isospin restoration (see Table II).

TABLE III. The nuclear matrix elements $M^{2\nu}_{\rm GT-1}$ and $M^{2\nu}_{\rm GT-3}$ calculated from measured $GT^{\pm}$ strengths in charge-exchange reaction (ChER) under the assumption of a equal phases for each individual contribution [29–32] and their product with squared effective axial-vector coupling constant $g_A^{\rm eff}$, which is determined within the single-state dominance hypothesis (SSD hypothesis) [13,14].

	SSD					ChER				
Nucleus	$(g_{\rm A}^{\rm eff})^2 M^{2\nu}_{\rm GT-1}$	$(g_{\rm A}^{\rm eff})^2 M^{2\nu}_{\rm GT-3}$	$(g_{\rm A}^{\rm eff})^2 M^{2\nu}_{\rm GT-5}$	$\xi^{2\nu}_{31}$	$\xi^{2\nu}_{51}$	$M^{2\nu}_{\rm GT-1}$	$M^{2\nu}_{\rm GT-3}$	$M^{2\nu}_{\rm GT-5}$	$\xi^{2\nu}_{31}$	$\xi^{2\nu}_{51}$
^{48}Ca						4.25×10^{-2}	2.31×10^{-3}	1.26×10^{-4}	0.054	0.003
^{76}Ge						8.61×10^{-2}	2.20×10^{-2}	5.61×10^{-3}	0.255	0.065
^{100}Mo	1.71×10^{-1}	6.29×10^{-2}	2.31×10^{-2}	0.368	0.135					
^{116}Cd	1.53×10^{-1}	4.57×10^{-2}	1.36×10^{-2}	0.298	0.089	5.88×10^{-2}	1.75×10^{-2}	5.22×10^{-3}	0.298	0.089
^{128}Te	1.60×10^{-2}	5.87×10^{-3}	2.16×10^{-3}	0.367	0.135					

D. Evaluation of effective axial-vector coupling constant

The calculation of $M^{2\nu}_{GT-3}$ can be more reliable than that of $M^{2\nu}_{GT-1}$ because $M^{2\nu}_{GT-3}$ is saturated by contributions through the lightest states of the intermediate nucleus. Thus, we rewrite the $2\nu\beta\beta$-decay rate as follows:

$$\left[T^{2\nu\beta\beta}_{1/2}\right]^{-1} \simeq \left(g_A^{\rm eff}\right)^4 \left|M^{2\nu}_{GT-3}\right|^2 \frac{1}{\left|\xi^{2\nu}_{31}\right|^2}\left(G^{2\nu}_0 + \xi^{2\nu}_{31} G^{2\nu}_2\right), \quad (39)$$

i.e., without explicit dependence on the matrix element $M^{2\nu}_{GT-1}$. For the sake of simplicity it is assumed that values of involved nuclear matrix elements are real. From Eq. (39) it follows that, if $\xi^{2\nu}_{31}$ is deduced from the measured $2\nu\beta\beta$-decay energy distribution and $M^{2\nu}_{GT-3}$ is reliably calculated by nuclear structure theory, the value of the effective axial-vector coupling constant $g_A^{\rm eff}$ can be determined from the measured $2\nu\beta\beta$-decay half-life.

Let us discuss the value of $\xi^{2\nu}_{31}$ within different approaches before it will be measured by the double-beta-decay experiment. Within the SSD hypothesis [13,14,21] it is supposed that the $2\nu\beta\beta$-decay NME is governed by the two virtual transitions: the first one going from the initial 0^+ ground state to the 1^+ ground state of the intermediate nucleus and second one from this 1^+ state to the final 0^+ ground state. Within this assumption we obtain

$$\left(g_A^{\rm eff}\right)^2 M^{2\nu}_{GT-k} \simeq m_e^k \frac{\left(g_A^{\rm eff}\right)^2 M_1}{\left(E_1 - \frac{(E_i - E_f)}{2}\right)^k} = \frac{3D}{\sqrt{f t_\beta f t_{EC}}} \frac{m_e^k}{\left(E_1 - \frac{(E_i - E_f)}{2}\right)^k}, \quad (40)$$

with $k = 1$ and 3. Here, $D = [3\pi^3 \ln(2)]/(G_\beta^2 m_e^5)$ is the beta-decay constant. The main advantage of the SSD approach is that the product $(g_A^{\rm eff})^2 M_1$ can be evaluated from the measured $\log ft$ values associated with the electron capture and single-β-decay of the ground state of intermediate nucleus with $J^\pi = 1^+$. There are three double-beta systems with $A = 100$, 116, and 128, which allow it. The corresponding SSD predictions for $(g_A^{\rm eff})^2 M^{2\nu}_{GT-k}$ ($k = 1$ and 3) and $\xi^{2\nu}_{31}$ are listed in Table III.

The Gamow–Teller strengths to excited states of intermediate nucleus from initial and final ground states entering the double-beta-decay transition are measured with help of charge-exchange reactions (ChER) [29–32], i.e., via strong interaction due to spin-isospin Majorana force. For ^{48}Ca, ^{76}Ge, and ^{116}Cd the calculated matrix elements $M^{2\nu}_{GT-1}$, $M^{2\nu}_{GT-3}$, and $\xi^{2\nu}_{31}$ under the assumption of equal phases for each individual contribution are presented in Table III. The CheR allow us to measure with a reasonable resolution of about tens of keV the Gamow–Teller strengths only up to about 5 MeV, i.e., below the region of the Gamow–Teller resonance, which might be considered as a drawback. We note that some questions arise also about the normalization of the Gamow–Teller strengths by the experiment.

The *pn*QRPA, SSD, and CheR predictions for parameter $\xi^{2\nu}_{31}$ for various isotopes are displayed in Fig. 10. We see that a best agreement among different results occurs by ^{116}Cd. In the case of ^{48}Ca and ^{76}Ge there is a significant difference between the *pn*QRPA and CheR results. We note that, within the HSD hypothesis [13,14], the value of $\xi^{2\nu}_{31}$ is equal to zero.

By considering the SSD values for $\xi^{2\nu}_{31}$ (see Table III) we obtain

$$g_A^{\rm eff}(^{100}{\rm Mo}) = \frac{0.251}{\sqrt{M^{2\nu}_{GT-3}}}, \quad g_A^{\rm eff}(^{116}{\rm Cd}) = \frac{0.214}{\sqrt{M^{2\nu}_{GT-3}}}. \quad (41)$$

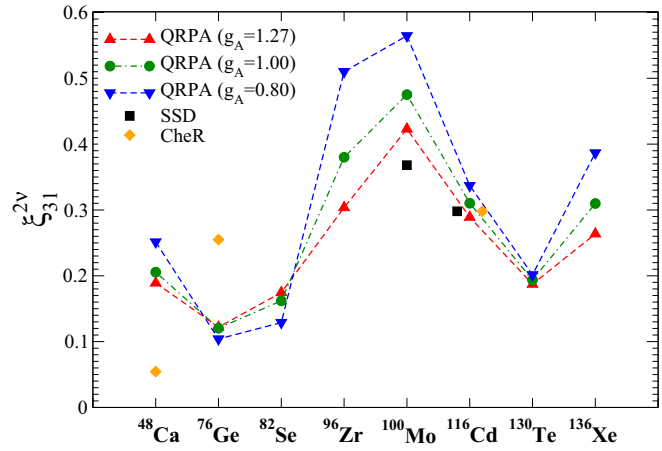

FIG. 10. The ratio $\xi^{2\nu}_{31}$ of nuclear matrix elements $M^{2\nu}_{GT-3}$ and $M^{2\nu}_{GT-1}$ calculated within the *pn*QRPA with partial restoration of isospin symmetry [24] by assuming $g_A^{\rm eff} = 0.80$, 1.00, 1nd 1.269, the single-state dominance hypothesis (SSD) [13,14], and by using the Gamow–Teller strengths measured in charge-exchange reactions (CheR) [29–32] under the assumption of equal phases of all contributions to the matrix element.

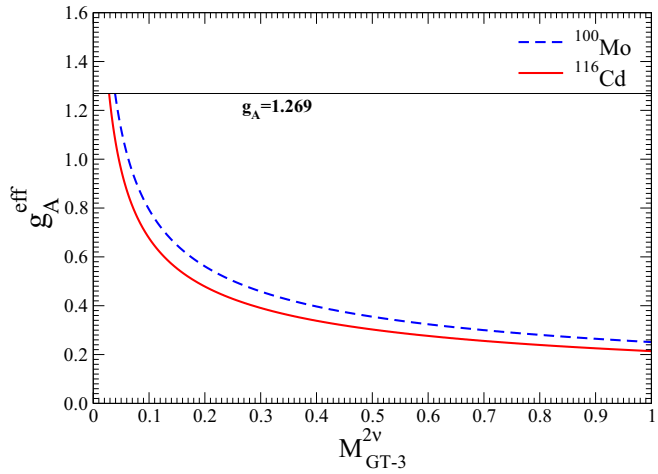

FIG. 11. The effective axial-vector coupling constant $g_A^{\rm eff}$ as function of the matrix element $M^{2\nu}_{GT-3}$ for $2\nu\beta\beta$-decay of ^{100}Mo and ^{116}Cd. The SSD values are assumed for $\xi^{2\nu}_{31}$ (see Table III).

The corresponding curves are plotted in Fig. 11. It is apparent that, if the value of $M^{2\nu}_{GT-3}$ were calculated reliably, e.g., within the interacting shell model, which is known to describe very well the lowest excited states of parent and daughter nuclei participating in a double-beta-decay process, one could conclude about the value of the effective axial-vector coupling constant $g_A^{\rm eff}$ for a given nuclear system. However, we note that the correct value of $g_A^{\rm eff}$ can be determined only if $\xi^{2\nu}_{31}$ deduced from the measured $2\nu\beta\beta$-decay energy distribution is considered. In that case the constant on the right-hand side of Eq. (41) might be different.

IV. SUMMARY AND CONCLUSIONS

In summary, improved formulas for the $2\nu\beta\beta$- and $0\nu\beta\beta$-decay half-lives are presented by taking advantage of the Taylor expansion over the parameters containing the lepton energies of energy denominators. The additional terms due to Taylor expansion in the decay rate have been found to be significant in the case of the $2\nu\beta\beta$-decay and practically of no importance in the case of the $0\nu\beta\beta$-decay.

Up to first order in the Taylor expansion the $2\nu\beta\beta$-decay rate includes two nuclear matrix elements $M^{2\nu}_{GT-1}$ and $M^{2\nu}_{GT-3}$ with energy denominators in the first and third power, respectively. It was shown that the ratio of these matrix elements $\xi^{2\nu}_{31} = M^{2\nu}_{GT-3}/M^{2\nu}_{GT-1}$ might be determined experimentally from the shape of the single and sum electron energy distributions, if the statistics of a considered double-beta-decay experiment allows it. A study of the SSD and HSD hypotheses in the case of the $2\nu\beta\beta$-decay of ^{100}Mo by the NEMO3 experiment has manifested that it is feasible [28].

A measured value of $\xi^{2\nu}_{31}$ is expected to constitute important information about virtual transitions through the states of intermediate nucleus. The calculation of the running sum of $M^{2\nu}_{GT-1}$ and $M^{2\nu}_{GT-3}$ performed within the pnQRPA with partial restoration of isospin symmetry showed that $M^{2\nu}_{GT-3}$ is determined by contributions through the low-lying states of the intermediate nucleus unlike $M^{2\nu}_{GT-1}$, which is affected significantly also by contributions through transitions over intermediate nucleus from the region of the Gamow–Teller resonance.

Furthermore, the $2\nu\beta\beta$-decay rate was expressed with $M^{2\nu}_{GT-3}$ and $\xi^{2\nu}_{31}$, i.e., without the explicit dependence on the commonly studied nuclear matrix element $M^{2\nu}_{GT-1}$. It was suggested that one can get information about the axial-vector coupling constant in nuclear medium $g_A^{\rm eff}$ once $\xi^{2\nu}_{31}$ is deduced from the measured electron energy distribution and $M^{2\nu}_{GT-3}$ is calculated reliably, e.g., within the ISM.

It goes without saying that an improved formula for the $2\nu\beta\beta$-decay half-life will play an important role in the accurate analysis of the Majoron mode of the $0\nu\beta\beta$-decay and in the study of Lorentz-invariance violation, bosonic admixture of neutrinos, and other effects.

ACKNOWLEDGMENTS

This work was supported by the VEGA Grant Agency of the Slovak Republic under Contract No. 1/0922/16, by the Slovak Research and Development Agency under Contract No. APVV-14-0524, RFBR Grant No. 16-02-01104, Underground Laboratory LSM - Czech participation to European-level research infrastructure CZ.02.1.01/0.0/0.0/16 013/0001733.

[1] W. C. Haxton and G. J. Stephenson Jr., Prog. Part. Nucl. Phys. **12**, 409 (1984).
[2] M. Doi, T. Kotani, and E. Takasugi, Prog. Theor. Phys. Suppl. **83**, 1 (1985).
[3] J. D. Vergados, H. Ejiri, and F. Šimkovic, Rep. Prog. Phys. **75**, 106301 (2012).
[4] A. S. Barabash, Nucl. Phys. A **935**, 52 (2015).
[5] D. Štefanik, F. Šimkovic, and A. Faessler, Phys. Rev. C **91**, 064311 (2015).
[6] V. A. Rodin, A. Faessler, F. Šimkovic, and P. Vogel, Phys. Rev. C **68**, 044302 (2003).
[7] V. A. Rodin, A. Faessler, F. Šimkovic, and P. Vogel, Nucl. Phys. A **766**, 107 (2006); **793**, 213(E) (2007).
[8] E. Caurier, F. Nowacki, A. Poves, and J. Retamosa, Phys. Rev. Lett. **77**, 1954 (1996).
[9] K. Muto, E. Bender, and H. V. Klapdor-Kleingrothaus, Z. Phys. A: Hadrons Nucl. **339**, 435 (1991).
[10] R. Arnold *et al.* (The NEMO-3 Collaboration), Nucl. Phys. A **765**, 483 (2006).
[11] A. S. Barabash, A. D. Dolgov, R. Dvornický, and F. Šimkovic, Nucl. Phys. B **783**, 90 (2007).
[12] J. B. Albert *et al.* (EXO-200 Collaboration), Phys. Rev. D **93**, 072001 (2016).
[13] F. Šimkovic, P. Domin, and S. V. Semenov, J. Phys. G **27**, 2233 (2001).
[14] P. Domin, S. Kovalenko, F. Šimkovic, and S. V. Semenov, Nucl. Phys. A **753**, 337 (2005).

[15] M. Agostini *et al.* (GERDA Collaboration), Nature (London) **544**, 47 (2017).
[16] R. Arnold *et al.* (The NEMO-3 Collaboration), Phys. Rev. D **92**, 072011 (2015).
[17] K. Alfonso *et al.* (CUORE Collaboration), Phys. Rev. Lett. **115**, 102502 (2015).
[18] N. Ackerman *et al.* (EXO Collaboration), Phys. Rev. Lett. **107**, 212501 (2011).
[19] A. Gando, Y. Gando, H. Hanakago, H. Ikeda, K. Inoue, R. Kato, M. Koga, S. Matsuda, T. Mitsui, T. Nakada, K. Nakamura, A. Obata, A. Oki, Y. Ono, I. Shimizu, J. Shirai, A. Suzuki, Y. Takemoto, K. Tamae, K. Ueshima, H. Watanabe, B. D. Xu, S. Yamada, H. Yoshida, A. Kozlov, S. Yoshida, T. I. Banks, J. A. Detwiler, S. J. Freedman, B. K. Fujikawa, K. Han, T. O'Donnell, B. E. Berger, Y. Efremenko, H. J. Karwowski, D. M. Markoff, W. Tornow, S. Enomoto, and M. P. Decowski (KamLAND-Zen Collaboration), Phys. Rev. C **85**, 045504 (2012).
[20] J. Barea, J. Kotila, and F. Iachello, Phys. Rev. C **91**, 034304 (2015).
[21] J. Abad, A. Morales, R. Nunez-Lagos, and A. Pacheco, Ann. Fis. A **80**, 9 (1984).
[22] J. Menendez, D. Gazit, and A. Schwenk, Phys. Rev. Lett. **107**, 062501 (2011).
[23] J. Engel, F. Šimkovic, and P. Vogel, Phys. Rev. C **89**, 064308 (2014).
[24] F. Šimkovic, V. Rodin, A. Faessler, and P. Vogel, Phys. Rev. C **87**, 045501 (2013).
[25] J. Kotila and F. Iachello, Phys. Rev. C **85**, 034316 (2012).
[26] F. Salvat, J. M. Fernandez-Varea, and W. Williamson Jr., Comput. Phys. Commun. **90**, 151 (1995).
[27] A. Giuliani and A. Poves, Adv. High Energy Phys. **2012**, 857016 (2012).
[28] R. Arnold *et al.* (NEMO-3 Collaboration), JETP Lett. **80**, 377 (2004).
[29] S. Rakers *et al.*, Phys. Rev. C **70**, 054302 (2004).
[30] E. W. Grewe *et al.*, Phys. Rev. C **78**, 044301 (2008).
[31] H. Dohmann *et al.*, Phys. Rev. C **78**, 041602(R) (2008).
[32] S. Rakers *et al.*, Phys. Rev. C **71**, 054313 (2005).